ISSN: 2573-9506

Review Article

International Journal of Women's Health Care

# Ionization Dosimetry Principles for Conventional and Laser-Driven Clinical Particle Beams

**F Scarlat[1,2*], E Stancu[2,3], E Badita[2], A Scarisoreanu[2], C Vancea[2,3], I Calina[2,3], M Demeter[2,4], Fl Scarlat[5] and R Chiru[6]**

[1]*Valahia University of Targoviste: Bd. Carol Street/2, Targoviste, Dambovita, Romania*

[2]*National Institute for Laser, Plasma and Radiation Physics, Atomistilor Str./409, Magurele, Ilfov, Romania*

[3]*University of Bucharest, Faculty of Physics, Atomistilor Street/407, Bucharest, Romania*

[4]*University of Bucharest, Faculty of Chemistry, Regina Elisabeta Street/4-12, 030018, Bucharest, Romania*

[5]*SC Bitsolutions SRL, Calea 13 Septembrie Street/201, Bucharest, Romania*

[6]*SC Medfam SCARLAT SRL, Bd. Ghencea/43 B, Bucharest, Romania*

**[*]Corresponding author**
Scarlat Florea, Valahia University of Targoviste: Bd. Carol Street/2, Targoviste, Dambovita, Romania, E-mail: scarlat.f@gmail.com

**Submitted**: 18 July 2018; **Accepted**: 24 July 2018; **Published**: 30 July 2018

## Abstract

*In this paper after mentioning the clinical radiation fields of 20 keV-450 MeV/u, they are characterized by the number of particles and their energy. Particle energy is the quantity that determines radiation penetration at the depth at which the tumor is situated (Fig. 1). The number of particles (or beam intensity) is the second major quantity that assures the administration of the absorbed dose in the tumor. The first application shows the radiation levels planned for various radiation fields. Prior to interacting with the medium, the intensity (or energy fluence rate) allows the determination of energy density, energy, power and relativistic force. In the interaction process, it determines the absorbed dose, kerma and exposure. Non-ionizing radiations in the EM spectrum are used as negative energy waves to accelerate particles charged into special installations called particle accelerators. The particles extracted from the accelerator are the source of the corpuscular radiation for high-energy radiotherapy. Of these, light particle beams (electrons and photons) for radiotherapy are generated by betatron, linac, microtron, and synchrotron and heavy particle beams (protons and heavy ions) are generated by cyclotron, isochronous cyclotron, synchro-cyclotron and synchrotron. The ionization dosimetry method used is the ionization chamber for both indirectly ionizing radiation (photons and neutrons) and for directly ionizing radiation (electrons, protons and carbon ions). Because the necessary energies for hadrons therapy are relatively high, 50-250 MeV for protons and 100-450 MeV/u for carbon ions, the alternative to replace non-ionizing radiation with relativistic laser radiation for generating clinical corpuscular radiation through radiation pressure acceleration mechanism (RPA) is presented.*

## Introduction

Radiation (from fr. Radiation) is a physical phenomenon of emission and propagation from waves (wave radiation) or corpuscles (corpuscular radiation).

According the principle of relativity requiring the force field and the quantum principle requiring quanta of the field, i.e. force carrier particles, the photon is the quantum of the classical electromagnetic field and a matter particle is the quantum of some kind of matter field.

This paper deals with photons - the mediators of electromagnetic interaction, electrons which are fundamental particles and have no discernable substructure, and hadrons containing quarks, for example: baryons (protons = 2 up quark + 1 down quark and neutrons =1 up quark +2 down quark) and mesons (=1 quark + 1 antyquarks) [1].

The electromagnetic radiation spectrum can be divided into two areas: non-ionizing electromagnetic waves that start from radio frequency and end up with ultraviolet and indirectly ionizing radiation including photons (X rays, gamma and bremsstrahlung).

Leptons (electrons and positrons) and hadrons (protons, ions of other atoms) with charge are directly ionizing radiation. Charged particles in interaction with a target generate photons of type: - bremsstrahlung (B) when target is a solid material, synchrotron radiation (SR) when

target is a magnetic field and - free electron laser radiation (FEL) when target is a periodic magnetic field.

After presenting the physical data of the three types of radiation (non-ionizing, indirectly and directly ionizing), the radiation field is characterized and then the characteristics of the hadron accelerators using radio frequency (RF) waves with wavelengths of the order of meters for particle acceleration are mentioned [2].

The depth dose distribution of the proton and carbon ions absorbed has the most appropriate profile in setting the patient's treatment plan due to the Bragg-Gray peak, which at the end of the range is about 4 times larger than the dose level to peak, Fig .1 [3].

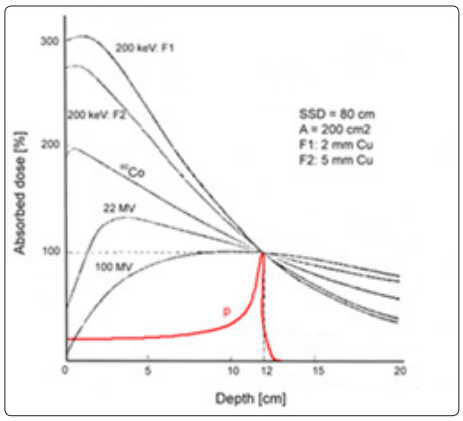


**Figure 1**. Depth dose in tissue for $^{60}$Co rays, X rays of 200 keV, photons of 22 MeV, 100 MeV and protons of 130 MeV

Also, some physical aspects of the interaction of particles with the environment related to ionization chamber dosimetry are presented [4-6].

Existence in the construction of high-power laser systems (10 PW) has reinforced the old idea of replacing the RF wave with relativistic laser wave to accelerate electrons and hadrons to the energies required by therapy: (50-250) MeV for protons and (100-450) MeV/u for carbon ions [7-9].

Dosimetric quantities for photons/electrons dosimetric are related to the energy fluence/particle fluence of the radiation field. It presents the calculation formalism for exposure, kerma and absorbed dose in the air and in the medium [10-13].

Determination of the absorbed dose is made in accordance with the charged particle equilibrium (CPE) principle in photon irradiation and the Bragg-Gray principle in irradiation with ionizing radiation [14-16].

## The Spectrum of Electromagnetic Radiation

The electromagnetic spectrum (Fig. 2) is described with respect to a characteristic wavelength (λ) and associated energy, $E_{\hbar\omega} \equiv \hbar\omega$, where $\hbar$ =1.055.10-34[J.s] is the smallest observable action value and ω= 2πc/λ), by relation:

$$E_{\hbar\omega}[eV] = \frac{1239.84\ nm \cdot eV}{\lambda[nm]} \quad (1)$$

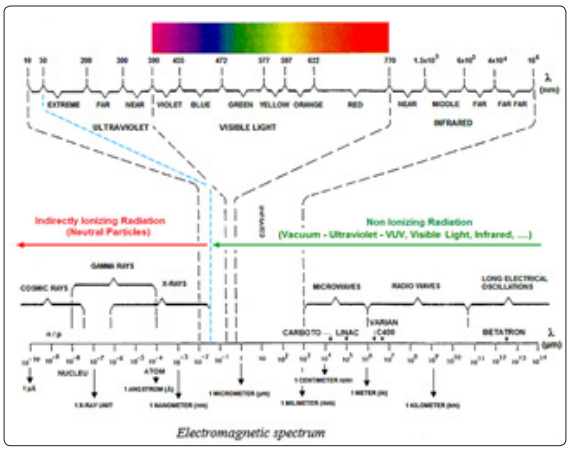


**Figure 2**: The spectrum of electromagnetic radiation [RCA Electro-Optics 1976]

It includes: thermal electromagnetic radiation (Stefan - Boltzman): $\hbar\omega > 2.22 \times 10^{-6}$ eV(1°K), radio waves: $1.23 \times 10^{-8} < eV < 1.23 \times 10^{-3}$, microwaves: $1.23 \times 10^{-6} < eV < 1.23 \times 10^{-3}$, infrared: $1.23 \times 10^{-3} < eV < 1.6$ eV, visible: $1.6 < eV < 3.2$, ultraviolet: $3.2 < eV < 123$), soft X rays: $123 < eV < 12.3 \times 10^{3}$, hard X rays: $12.3 \times 10^{3} < eV < 1.23 \times 10^{6}$, radiatia gamma: $1.23 \times 10^{6} < eV < 1.23 \times 10^{17}$ and cosmic radiation, $\hbar\omega > 1.23 \times 10^{17}$eV.

The radiation spectrum analysis shows that it has two distinct regions. The first region represents nonionizing electromagnetic waves (or nonionizing radiation), which begins with black body radiation and ends with ultraviolet radiation (UV). The second region is indirectly ionizing radiation. This starts with soft X rays (SXR) radiation and continues with cosmic radiation.

CNCAN NSR 01 Norms in Romania state that indirect ionizing radiation for electrical equipment operating a potential difference over 5 kV generates indirect ionizing radiation. Its energy ħω corresponds to the associated wavelength λ = 0.248 nm. Up to this limit, radiation is treated as a nonionizing electromagnetic wave.

## Nonionizing Electromagnetic Wave

A radiation that is not as energetic as ionizing radiation and cannot remove electrons from atoms or molecules.

Nonionizing radiation encompasses regions: ultraviolet or UV (near, far, extreme), defined as the wavelength range ($10 \leq \lambda < 380$) nm, Visible - VIS ($380 \leq \lambda < 760$) nm, infrared - IR ($760 \leq \lambda < 10^{6}$) nm, microwave - MW (1 mm ≤ λ < 1 m), radio waves – RW (1 m ≤ λ < 100 m) and long electrical oscillations (λ >100 m), according RCA Electro-Optics 1976.

In nature there is the principle that "Any body of nature with a temperature above 0 $^{0}$K emits thermal radiation in space under electromagnetic waves". The thermal energy emitted by the matter in thermodynamic equilibrium is related to the body temperature that emit the radiation through the relation $E_{\hbar\omega}$ = kT; where k = 1.38x10-23 J /K is Boltzman's constant, which indicates the lowest value of entropy in nature (S ≥ k).

Using the relation $E_{\hbar\omega}$ = kT, the following temperatures are obtained in degrees Kelvin – K, (T [K] = T [$^{0}$C] + 273.15) for non-ionizing EM waves: radio wave - $1.44 \times 10^{-2} \geq K > 1.44 \times 10^{-4}$, microwave

- 14.4 ≥ K >1.44 x $10^{-2}$, infrared 1.9 x $10^4$ ≥ K >14.4, Visible - 3.79 x $10^4$ ≥ K > 1.9x$10^4$ and UV -1.44 x $10^6$ ≥ K > 3.79x$10^4$ .

To date, MW, RW and LEO electromagnetic waves are used as negative energy waves in special devices called particle accelerators charged to obtain corpuscles radiation. Particles accelerated to the energy required for a particular application, are extracted from the accelerator, or are focuses on a metal target with large atomic number (Z) for generating braking radiation.

Among RF waves used in accelerators, we mention some values as a size order: 50 Hz for betatron (Kerst 1940), linear accelerator (3 GHz), microtron (3 GHz), cyclotron (80 MHz), syncrocycloton (150 MHz), isochronous cyclotron (75MHz) and synchrotron (100 MHz) [2].

In the present, there are a series of acceleration mechanisms with the laser technology (TNSA, RPA and others) using the relativist laser (I > $10^{18}$ W/cm$^2$) to generate proton clinical beams (50 - 250 MeV) and $^{12}$C ions (100 - 450) MeV/u.

Non-ionizing EM waves are characterized by intensity of radiation I (called the energy fluency rate in ICRU). This is achieved by averaging the Poynting vector over one wave cycle,

$$I\ [W/m^2] \equiv <S> = c\varepsilon_0 Em^2/2, \qquad (2)$$

where c = 2.99792458 x $10^8$ m/s, is the speed of light in vacuum, $\varepsilon_0$ = 8.854x$10^{-12}$A.s/V.m is the permittivity of vacuum, and $E_m$ is the electromagnetic wave amplitude.

We mention some non-ionizing radiation intensities:- the black body radiation: T = 300 °K (26.85 °C), 2.583x$10^{-2}$ eV) → 429.27 W/m$^2$, 6.19 x $10^{-6}$ J/m$^3$ ; - solar radiation: 1322 W/m$^2$, (41-4130) eV; treatment laser radiation (He-Ne), 1mW, 632.8 μm → 620 W/m, - cellphone: 100 kHz - 7 GHz, (0.41x$10^{-9}$ - 2.89x$10^{-5}$) eV, 0.78x$10^2$ W/m$^2$ < 2 W/m$^2$ and 2.42 V/m < 38.77 V/m [3].

Reference levels at frequency (electric field E strength [V/m], magnetic field H strength [A/m], B fied [μT] and equivalent plane wave density S[W/m$^2$]) for general public exposure/occupational public exposure, are the following: 10 - 400 MHz (28/61, 0.073/0.16, 0.092/0.2, 2/10) and for 2 -300 GHz (61/137, 0.16/0.36, 0.20/0.45, 10/50). These values are selected from the International Commission on Non-Ionizing Radiation Protection (ICNIRP [17].

The depth of penetration for tissues with high water content is 0.413 cm (8 GHz; 3.3x10-5 eV) and 0.343 cm (10 GHz; 4.13x$10^{-5}$ eV) [18].

## Indirectly Ionizing Radiation

A radiation that has sufficient energy to remove electrons from atoms or molecules as it passes through matter. Examples: photons, neutrons and other uncharged particle.

By introducing the photon energy $E_{\hbar\omega}$ = pc and the rest mass $E_0$ = $m_0c^2$ in the relation energy-impulse, $E^2 = E_0^2 + p^2c^2$, the mass of the photon equals zero. In other words, when $E_{\hbar\omega}$ = pc a "particle" does not have a rest mass. Particles without mass do not have a rest frame of reference. They are moving at the speed of light in any frame of reference. Waves are pure energy.

The main characteristics of photon interaction with matter are: high energy transfer to direct ionizing radiation, the absorbed dose is given by direct ionizing radiation and the camera-detector response is given by the interaction of the photons with the air in the detector cavity and the fluence has exponential attenuation.

The depth dose distributions for photon energies of 6 MV and 20 MV (Mevatron KD) and 6 MV and 18 MV (Therac 20) are presented in Fig.3 [19].

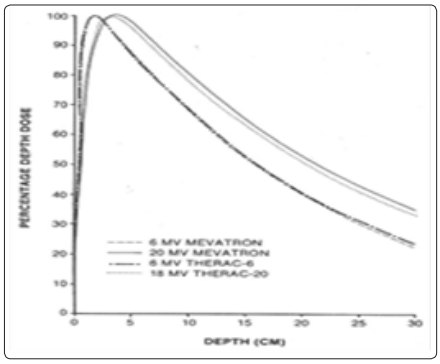


**Figure 3**: Central axis depth dose data: 10x10 cm$^2$ field size, 100 cm SSD measured in water for the 6- and 20 -MV photon beams [19].

In this figure the general shape of the photon depth dose curve is presented. Absorbed dose measurements take place in a V volume of the ionization chamber centered at the depth $x_m$ at which the dose has the maximum value. Charged particle equilibrium (CPE) is said to exist at a point M, centred in a volume V, at depth $x_m$, if each charged particle carrying out a certain energy from this volume is replaced by another identical particle which carrying the same energy into the volume.

Mathematically, CPE exists when the divergence of the charged particle beam energy fluence vector is equal to zero, $div\Psi_{CPE} = 0$. In this case the dose D is equal to the collision kerma $K_{col}$, $D = K_{col}$ for (g = 0).

In the case of indirectly ionizing radiation, the calculation relation for the radiation intensity is given by the expression

$$I\ [MeV/cm^2s] = 0.912x10^6\ X / (\mu_{en}/\rho)_a \qquad (3)$$

where X is the exposure in air (a) in units of roentgen per minute [R/m] and $(\mu_{en}/\rho)_a$ is the mass energy absorption coefficient expressed in units of [cm$^2$/g] [14].

At indirectly ionizing radiation, add the laser ($\hbar\omega \approx 1.5$ eV) with intensity I [W/cm$^2$] higer than atomic intensity $I_A$ corresponding to the electric field $E_B$ that binds the electron to its atom. Using the bilding electric field $E_B = (e/4\varepsilon_0 r_B^2) = 5.1 \times 10^9$ V/m, with e the electron charge, $\varepsilon_0$ the dielectric constant, and Bohr atom radius $r_B = \hbar^2/me^2 = 5.3 \times 10^{-9}$ cm, result the atomic intensity $I_A = \varepsilon_0 cE_A^2/2 = 3.51 \times 10^{16}$ W/cm$^2$, which is the intensity of laser at which any target material will be ionized solely by the laser electric field [20].

Also, the free electron laser (FEL) is added which, depending on the electron beam energy, $E = \gamma.m_0c^2$, between 10 to 20 GeV, the undulator wavelength $\lambda_u$ and the deflection parameter K. These generate SXR photons with wavelength $\lambda_0$ given by:

$$\lambda_0 = \frac{\lambda_U}{2\gamma^2} \cdot (1 + K^2/2) \quad (4)$$

We mention the projects in this regard: The European X-Ray Laser Project XFEL (Germanny, E = 17.5 GeV, $\lambda_0$ = 0.1 nm), The Linac Coherent Light Source LCLS (USA, $E_b$ = 14.35 GeV, $\lambda_0$ = 0.15nm) and Spring 8 Compact SASE SCSS (Japan XFEL, $E_b$ = 6.135GeV, $\lambda_0$ = 0.1 nm) [21].

Thomson scattering of a laser ($\lambda_0$) to a relativistic electron beam ($E_b$) can be a compact laser synchrotron source (LSS) [22] of X ray with the photon energy ($E_{\hbar\omega}$) given by

$$E_{\hbar\omega}\,[\text{keV}] = 1.9\text{x}10^{-2}.E_b^2[\text{MeV}]/\lambda_0\,[\mu\text{m}]. \quad (5)$$

For $E_b$ = 30 MeV [23] and the interaction length L= $(2R.r_b)^{1/2}$, R-betatron radius and $r_b$ – electron beam radius, result: $\hbar\omega$ = 17 keV and

$$\lambda_0 = 1.24/E_{\hbar\omega}\ [\text{keV}] = 0.07\ \text{nm}. \quad (6)$$

Synchrotron radiation can generate photons of 17 keV, using an electron beam with energy $E_b$ = 5.18 GeV, an undulator with $\lambda_U$ = 1 cm and K = 1. The electron beam energy $E_b$ [24] is obtained with relationship (7)

$$E_{\hbar\omega}\,[\text{keV}] = 0.95\ E_b^2\ [\text{GeV}]/\lambda_U[\text{cm}](1+K^2/2) \quad (7)$$

The Thomson scattering of a $\lambda_0$ = 1μm incident laser beam off a relativistic electron beam with energy $E_b$ = 5 GeV can generate photon X rays of energy $\hbar\omega$ = 510 MeV.

The photon energies used in the clinical field are: - Grentz < 20 keV, - contact [20-50 keV]: mammography 22-40 keV, - superficial [50-150 keV]: radiography/fluoroscopy [50-100keV], dental interventional radiology 50-120 keV, general radiography 60-150 keV, and computer tomograph CT 100-150 keV, - orthovoltage [150-300 keV], - photon therapy [4-25 MeV] - Gamma rays therapy: - $^{60}$Co 1.25 MeV, - $^{137}$Cs 662 keV, $^{125}$I &$^{103}$Pd [20-35] keV and - neutron therapy [1 - 20 MeV].

## Directly ionizing radiation

Direct ionizing radiation consists of charged particles. The energy absorption per unit mass (dose) is mainly due to the phenomena of ionization and excitation. The response of the electron detector ionization chamber, which complies with the Bragg-Gray principle, is determined by the fluence of electrons released into the medium.

The main feature of directly ionizing radiation in interction with the medium is given by the range defined for leptons and hadrons, and especially the Bragg-Gray peak for hadrons (protons, antiprotons, carbon ions, alpha particles, etc.), Fig.4 [14].

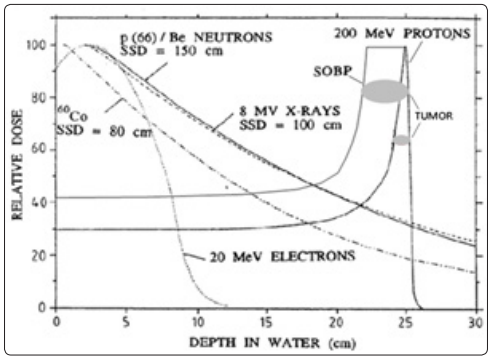


**Figure 4**: Physical characteristics of charged particle beams: 20 MeV- electron and 200 MeV proton

The important physical parameters of the charged particles are: the kinetic energy T, which determines their trajectory in the matter and the particle intensity I, which ensures obtaining the necessary dose for tumor sterilization or for radiography.

The electron beam provided by a linac, radiating a medium, in point of interest, absorbed dose rate is determined using the relationship Bragg-Gray,

$$D_m\,[\text{Gy/s}] = 1.6022\text{x}10^{-10}\phi.\ (S/\rho), \quad (8)$$

Where ϕ is the electron fluence rate in traditionale units [e/cm$^2$s] si S/ρ is the stopping power of energy in [MeVcm$^2$/g].

Directly ionizing radiation has many areas of application, of which we mention: - electron therapy [4-25 MeV], - proton therapy [50-250 MeV], - heavy ions therapy [100-450 MeV/u], - meson therapy (supplying photons /electrons) 500-700 MeV, - electron beam angiography 500-1000 MeV, - electron beam computed tomography [MeV], - protons/ neutron production/therapy tens of MeV, sterilization, food preservation 2-10 MeV, - α emitters [4-9 MeV], - deuterons/radioisotope production 7-20 MeV, - protons/ radioisotope production 10-100 MeV [3].

To take a clinical treatment of a malignant tumor with a beam of photons of 10 MeV, $(\mu_{en}/\rho)_a$ = 0.0150 cm$^2$/g, $\dot{X}$ = 1 R/m, 9.7x10$^{-6}$ W/cm$^2$ per R/m, and energy density of $U_{10}$ =3.23x10$^{-10}$ J/m$^3$. For administration of 10 Gy/weak, 2 Gy/day, with the absorbed dose of 1 Gy/m, is obtained a radiation pressure for $\hbar\omega$ = 10 MeV, in the standard input field A = 10x10 cm$^2$, of 3.68 x10$^{-8}$ [N/m$^2$] < 4.51x 10$^{-6}$ [N/m$^2$] (solar pressure). The photon beam power propagating at the speed of light is P = 0.11 W < 13 W (solar power) and the force F acting on the A radiation field is F= 3.68 x 10$^{-10}$ N < 4.51x10$^{-8}$ N (solar force) [3].

## Characterization of the ionizing radiation field

The radiation field is characterized by quantities based on the number of particles (N) and their energy, $E_{\hbar\omega}$ = ħω for photons and $E_{\hbar\omega}$ = T - kinetic energy for particles, both expressed in SI in [J] or in traditional units [MeV].

Of the radiation fields used in dosimetry we mention two quantities. The first is the charged or uncharged particle fluence [m$^{-2}$] = φ.t, which represents the number of particles per unit area. In the case of the Bragg-Gray chambers, this represents the fluence of the

secondary electrons in the environment and multiplied by the stopping power determines the absorbed dose.

The second quantity is the particle energy fluency, $\Psi$ [J.m$^{-2}$] = $\mathcal{E}.\Phi$ = $\psi$.t, defined as the particle energy per unit area. This is the size is used for determination of the three dosimetric quantities (absorbed dose, kerma and exposure) in case of medium irradiation with a photon beam. The sizes of $\varphi$ [m$^{-2}$s$^{-1}$] and $\psi$ [J.m$^{-2}$s$^{-1}$] represent the particle fluence flow and the particle energy flow rate.

When charged or uncharged particle beams are polyenergetic, particle fluence and energy fluence are replaced with the particle fluence spectrum, $\Phi_E = d\Phi(E)/dE$, and the energy fluence spectrum $\Psi_E = d\Psi(E)/dE = (d\Phi(E)/dE)xE$.

## Clinical hadron accelerators

Heavy particle clinical beams are currently generated by two types of accelerators: classic cyclotron as synchrocyclotron and isochronous cyclotron and synchrotron. In 2012, of about 12,000 accelerators in medicine, only 39 work for proton and ion therapy [25].

## Classical Cyclotron

The operating principle of classical cyclotron is shown in Figure 5 (Lawrence 1932) [26].

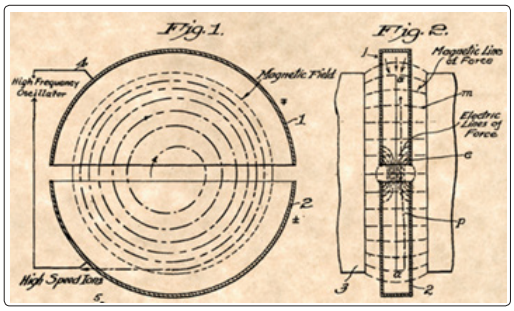


**Figure 5**: Front and profile view of patented cyclotron by E.O. Lawrence, US Patent Office [26].

The particles injected by a source located at the center of the magnet are accelerated on a spiral trace by the RF electrical voltage applied between two dees located inside a vacuum chamber, which in turn is located in the space between two magnetic poles providing the magnetic field with axial symmetry.

Ions when passing through the dees interval receive energy from the RF voltage, ($V=V_0 \cos \omega_{RF} t$). The transfer of energy from the electric field to the particle takes place based on the resonance phenomenon between the rotation frequency of the ion, $\omega_0 = 2\pi f_0$, and the frequency of the RF voltage, $\omega_{RF} = 2\pi f_{RF}$, during the acceleration period.

From equality of Lorentz force (qvB) with centrifugal force ($mv^2/R$) at a point in equilibrium orbit, result the expression for the particle frequency $\omega_0 = qB/m_0$. When the energy of the particle increases due to the increase of the particle mass $m_0$ with the relativistic factor $\gamma = (1-\beta^2)^{-1/2}$, $\beta \equiv v/c$, the particle frequency $\omega_0 \neq \omega_{RF}$ and the resonance phenomenon disappears.

By fixing a particle velocity value $\beta = v/c \leq 0.203$, $\gamma = 1.02$ at which the resonance disappears, results that the cyclotron's acceleration is limited to 20 MeV, in the case of protons. There have been a series of changes to the classic cyclotron to overcome this energy limit.

## Synchrocyclotron

In the relativist case ($\gamma > 1$), when $m = m_0\gamma$, and $\omega_0 = qB/m_0\gamma$, there are two acceleration versions. In the first version, the magnetic field $B = m_0\gamma\uparrow$. $\omega_{RF}\downarrow /q = \text{const}$ is constantly maintained, and the cyclotron frequency is decreased by means of a frequency modulation device to equalize it with the frequency of rotation of the particle.

The frequency modulated (FM) cyclotron or the synchro-cyclotron maintains the original cyclotron principle with a spiral particle path [27].

**Figure 6**: Synchrocyclotron Monarch 250 MeV, protons, 9T field, weight 20 tons with 9 T field [28].

The synchrocyclotron works on the principle of phase stability (Veksler '44, McMillan'45) which states that the ions would stay in phase with the RF, oscillating around a "synchronous phase" $\varphi_s$. Whereas the cyclotron can accelerate a stream of particles, the synchro-cyclotron can only accelerate "one bunch" of particles.

For proton therapy the Still Rivers Company conducted a Synchrocyclotron supraconductor (B = 9 T) of 250 MeV (Monarch 250) with a weight of 20 tons, Fig. 6 [28].

La Gatchina near St. Petersburg operates a 1000 MeV synchrocyclotron with standard magnets (B = 1.8 T) and weight of 10.000 tons (= weight of the Eiffel Tower).

**Isochronous cyclotron** is the second version of the classic cyclotron which maintains the constant frequency $\omega_0 = qB\uparrow/m_0\gamma\uparrow = \text{const.}$, and the increase of the magnetic field is synchronized with the mass increase.

This type of cyclotron works on the principle of alternating focusing (Christofilios1950). In the isochronous cyclotron, the magnetic field has a periodic spatial variation (azimuthal and radial, Kerst 1955) that provides the particle with a non-circular orbit.

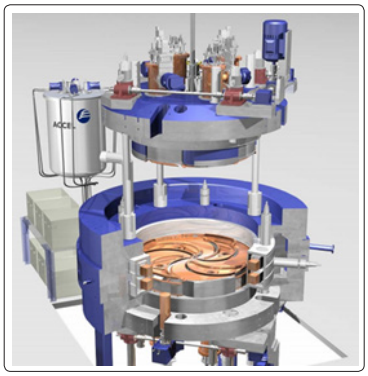

**Figure 7**: Periodic spatial variation of magnetic field at Varian 250 MeV SC Compact Proton Cyclotron [29]

In Fig. 7 is seen the strong and weak alternating magnetic azimuth regions (Sectors of "hills" and "valleys") in the isochronous cyclotron Varian SC 250 MeV [29].

We mention in this regard isochronous cyclotrons: IBA 235 proton therapy cyclotron (RF 106 MHz, NC coil: 1.7-2.2 T, 220 tons); VARIAN 250 MeV superconducting compact proton cyclotron (72.8 MHz, 2.4 – 3 T, < 90 tons) and IBA-JINIR C 400 carbon/proton therapy cyclotron (protons (260 MeV) and carbon ions (400MeV/u), 75 MHz, B= 2.45-4.5 T, 660 tons [30].

## Synchrotron

This change operating principle of cyclotron by replace the electrodes with smaller RF cavity (see Fig.8).

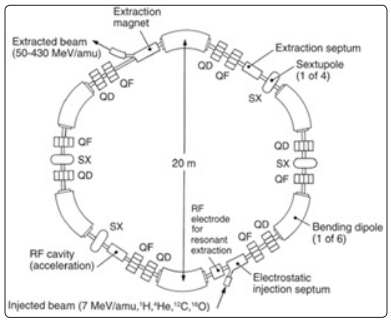


**Figure 8**: Configuration of Siemens ion synchrotron [31]

To obtain an equivalent circular orbit, particle injection into the synchrotron is done with a low energy accelerator. The synchrotron keeps the radius of the circle constant by increasing the strength of the magnetic field according to the relation R = p↑/0.3B↑ = const.

Mention for proton therapy and carbon therapy synchrotroanes of type: HIT, LLLMC, Siemens, Hitachi, Mitsubishi and Toshiba.

Currently, for radiotherapy, there are RD accelerators cyclinac (cyclotron + linac), fixed field alternating gradient accelerator - FFAG and dielectric wall accelerator - DWA using cyclotron technology with RF [2].

Replacing the RF (100 MHz, λ =300m) wave with laser wave (λ = 1μm =$10^{-6}$ m) in the acceleration process and the magnetic field from the irradiation head (about 120-600 t) by the use of the channelling phenomenon in the bent crystals can reduce the dimensions of these accelerators and increase the multiplication factor of medical facilities to allow more patients to access therapy [32-35].

## Laser-driven clinical hadron beams

Fig. 9 shows the second version of the laser accelerator in the article [9] when the target is located directly in the treatment room.

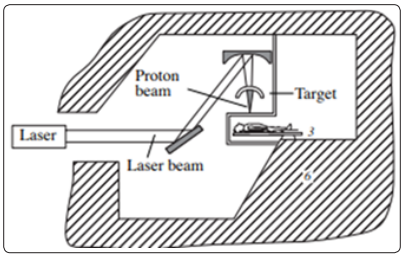


**Figure 9**: Laser driven proton therapy accelerator developed by Bulanov and Khoroshkov [9].

The laser beam (10 PW, 15 fs, 150 J, $10^{23}$ W/cm$^2$) generated by Apollo Laser System, now under construction on Magurele Platform near Bucharest, can be used for technological research on the parameters of an clinic laser accelerator [36-37].

Figure of merit of the laser system is the dimensionless intensity parameter of EM wave (ω = c.k) of amplitude $E_m$, $a_0 \equiv eEm / mc\omega$, related to the peak intensity of laser I through

$$a_0 = \sqrt{I \cdot \lambda^2 / (\xi \cdot 1.37 \times 10^{18})} \qquad (9)$$

In relatia (9), I [W/cm$^2$] = $E_L/\tau.A_{eff} = P_p/A_{eff}$, $E_L = P_p.\tau$ is the pulse energy, $P_p$ is the peak power, $A_{eff} = w_0^2/2 = 20.\lambda^2$[μm$^2$] is the laser beam cross-section, τ is the pulse time, $w_0$ is the radius of the laser beam at focus, $E_p = (2\ Z_0 P_p/A_{eff})^{1/2}$ is the peak electric field, $Z_0$ = 377 Ω is the free space impedance and ξ = 1/2 for linearly/circularly polarized laser.

The relativistic regime for electrons reaches at radiation intensity of I ≥$10^{18}$W/cm$^2$ (or $a_0$ >1), and for protons and carbon ions at I ≥ 5x$10^{24}$ W/cm$^2$ (or $a_0$ >1836). In this regime the laser system can provide X-ray and XUV beams,

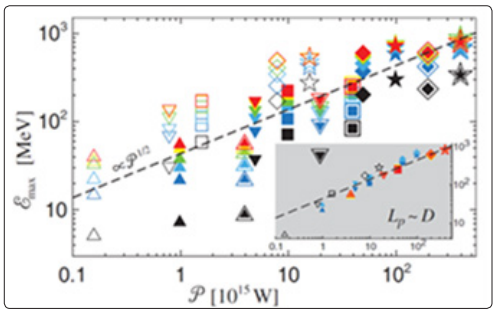


**Figure 10**: Proton maximum energy vs laser pwer for optimal plasma slab thickness [39]

Figure 10 shows the maximum energy of the proton $\mathcal{E}_{max}$ [MeV] according to the laser for $n_e$ =100 $n_{cr}$, the laser pulse length of the order of the focal spot size, $L_p$ =D, for various ratio D/λ, $L_p$/λ and intensities I = $10^{20}$-$10^{22}$ [W/cm$^2$] [38-39].

The interpretation of the data in Figure 3 obtained in the RPA LS acceleration regime [30] indicates that the proton energy is proportional to the square root of the intensity for thin targets, $\mathcal{E}_{max} \approx P^{1/2}$.

For use in hadron radiotherapy, schemas based on TNSA, RPA and other relativistic acceleration mechanisms are being researched and experimented ($a_0$ > 1) [40-41].

## Interaction of Photons with Matter

### Major Processes

The main local processes through which photons of energy $\mathcal{E}=\hbar\omega$ interact with the substance will be energy absorption and scattering [42-45].

The photoelectric effect (PE) takes place when the incident photon of energy $\hbar\omega$ interacts with an electron located on one of the orbits of the atom, with the energy of the bending B. The incident photon yields the energy B to extract the electron from the atom and the

rest of the incident photon energy T = ħω - B remains as the kinetic energy of the emerging electron. This process takes place when ħω > B. The effect PE is characterized by the mass absorption coefficient, denoted by τ/ρ and expressed in [$m^2$/kg] or in traditional units [$cm^2$/g].

The Compton Effect (CE) occurs when the energy photon interacts with the free or lightly bound electron. In this interaction process, the photon yields only a portion of the energy that, after interaction, a photon is scattered at a certain angle and with energy ħω"'. The released electron, called the Compton electron, has the mean kinetic energy $T_{av} = (\hbar\omega - \hbar\omega'')_{av} = (\sigma_a/\sigma)\hbar\omega$. The average energy of the scattered photons is $(\hbar\omega'')_{av} = \hbar\omega - T_{av} = \sigma_s = (\sigma_s/\sigma)\,\hbar\omega$). The CE effect is characterized by the Compton total mass attenuation coefficient, σ/ρ. This the sum of the mass absorption coefficient and the mass scatter coefficient, $\sigma/\rho = (\sigma_a + \sigma_s)/\rho$.

Producing electron pairs (PP) of electrons (e- , e +) is energy absorption. This occurs when the ħω energy photons interact with the nucleus field, provided that the incident photon energy is greater than 1.02 MeV (= $2m_0c^2$). The law of energy conservation is written in this case, $\hbar\omega = (m_0c^2 + T_+) + (m_0c^2 + T_-)$, which means that the two electrons have the energy difference ($T_+ + T_- \geq \hbar\omega - 2\,m_0c^2$). The photon has no rest mass, and the electrons with the rest mass, the creation of the two electrons rests mass, takes place according to the principle of Einstein's mass and energy equivalence. The effect PP is characterized by the mass absorption coefficient, κ/ρ, [$cm^2$/g].

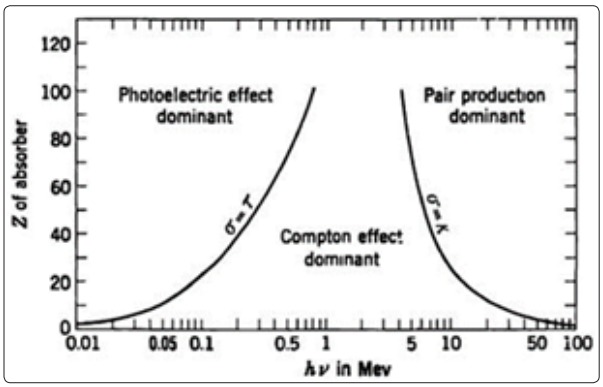


**Figure 11**: The three major types of gamma ray interaction: photoelectric effect, Compton Effect and pair production [46].

The three major effects produced by the interaction of the photon beam with medium are represented in Fig.11 [46]. The curves show the values of the atomic number Z and the energy of the photon ħω for which the neighbouring effects are equal.

Secondary photons and electrons can produce tertiary radiation (photon or electron δ) by ionisation or excitation outside the absorbed dose computation area.

## Photon interaction coefficients

In the area where the three major processes occur, the energy transfer from the incident-primary photon to the secondary electrons (photoelectrons, T, electrons Compton, Tave, and electron pairs, ($T_- + T_+$) occurs. When the photoelectron is released, the atom remains positive with a certain electronic hole.

Therefore, the total mass absorption coefficient is $\mu_a/\rho = \tau/\rho + \sigma a/\rho + \kappa/\rho$ and the total mass scattering coefficient is $\sigma i/\rho = \sigma_s/\rho + \sigma_R/\rho$, where $\sigma_R/\rho$ is the mass coherent scattering coefficient on bound electrons. When the Compton mass scattering coefficient $\sigma_s/\rho$ is added to $\mu_a/\rho$, we obtain the total linear attenuation coefficient:

$$\mu/\rho = (1/\rho)\,(\mu_a + \sigma_s) = (1/\rho)(\tau + \sigma_a + \sigma_s + \kappa) \qquad (10)$$

Because the Rayleigh scattering is elastic and is confined to small angles, it is not included in μ/ρ.

## Exponential Attenuation

Equation which describing the exponential attenuation of a photon beam intensity by absorption and scattering is,

$$I = I_0.e^{-\tau x}.e^{-\sigma x}.e^{-\kappa x} = I0e^{-\mu x} \qquad (11)$$

Where $I_0$ is the intensity of the incident photon beam or incident energy fluence rate, I(x) is the intensity after traversing a distance x through the absorbing medium, τ, σ and κ are the corresponding linear coefficients for photoelectric, Compton and pair production, and μ is the total linear attenuation coefficient. In equation (11), for simplicity, the density ρ was not introduced in the exponent because it disappears at each exponent, so: $\mu_x = (\mu/\rho).(x.\rho)$.

## Energy Transfer and Energy Absorption Coefficients

For dosimetric purposes, it is necessary to know the energy transferred from photons to secondary electrons as a result of the initial interaction. The mass energy transfer coefficients ($\mu_{tr}/\rho$) allow calculating this energy as a fraction f of the μ/ρ mass linear attenuation coefficient that refers, as follows: $\mu_{tr}/\rho \equiv (\mu/\rho).f = (\mu/\rho).(T_{av}/\hbar\omega)$, where $T_{av}$ is the average energy transferred from the primary photons of energy ħω to charged particles ($e^+$, $e^-$) as the kinetic energy T.

The mass energy transfer coefficients for the three major effects are obtained by eliminating the average energy fraction emitted for: generating characteristic X-ray radiation, generating the Compton scattered photons, and the energy that contributes to radiation annihilation.

Finally, the mass energy transfer coefficient is obtained

$$\frac{\mu_r}{\rho} = \frac{\tau}{\rho}\left(1 - \frac{\delta}{\hbar\omega}\right) + \frac{\sigma}{\rho}\left(\frac{T_{avg}}{\hbar\omega}\right) + \frac{\kappa}{\rho}\left(1 - \frac{2m^2}{\hbar\omega}\right) \qquad (12)$$

By eliminating the energy of the secondary electrons consumed to generate the radiation bremsstrahlung, we obtain expression for the linear mass energy absorption coefficient, $\mu_{en}/\rho$

$$\frac{\mu_{en}}{\rho} = \frac{\mu_{tr}}{\rho}(1 - g) \qquad (13)$$

where g is the fraction of energy lost by secondary electrons (photoelectrons, Compton electrons and pair of electrons) in bremsstrahlung. From the balance of energy, it results $(\hbar\omega)_{tr} = (\hbar\omega)_{en} + g.(\hbar\omega)_{tr}$ or written otherwise

$$g = \frac{(\hbar\omega_{tr} - \hbar\omega_{en})}{\hbar\omega_{tr}} \qquad (14)$$

For the energies used in diagnostic radiology, g may be taken as zero. The value (1-g) slowly decreases with increasing photon energy.

Because of their importance as gamma calibration sources for dosimetry, exact values of (1–g) have been determined for $^{137}$Cs photons ($\hbar\omega = 0.662$ MeV) and $^{60}$Co photons ($\hbar\omega = 1.332$ and 1.172 MeV) to be 0.9984 and 0.9968, respectively [44].

## Exposure, Kerma and Absorbed Dose in Air

Expunerea, X, is a measure of ionization per unit mass irradiated produced in air by X or gamma radiation. $X[R] \equiv dQ/dm = \Psi/\Psi_R$, is ratio between the energy fluence ($\Psi = 1.6022 \times 10^{-6}\ \Phi.\hbar\omega$ [erg/cm$^2$]) and incident energy fluence per roentgen ($\Psi_R = 87.64/(\mu_{en}/\rho)_a$ [erg/cm$^2$R] ;1R =2.58 x 10$^{-4}$C/kg).

The exposure at the point of interest is given by the relation:

$$X[R] = 1.827 \times 10^{-8}.\hbar\omega.\phi.\ (\mu_{en}/\rho)_a \qquad (15)$$

Exposure and exposure rate apply only to X-rays and gamma rays up to energies of about 3 MeV and only in air.

**Kerma in air, $K_a$**, is the photon energy transferred per unit mass to electrons by photons. $K_a[Gy] = d(\hbar\omega)_{tr}/dm = \Psi.(\mu_{tr}/\rho)_a$. It can be calculated by the incident photon energy fluence so

$$K_a[Gy] = 1.6022 \times 10^{-10} \cdot \Phi \cdot \left(\frac{\mu_{en}}{\rho}\right)_a \cdot \frac{\hbar\omega}{1-g} \qquad (16)$$

**Absorbed dose, $D_a$**, is a measure of energy deposition per unit mass irradiated. $D_a\ [Gy] = \Psi.(\mu_{en}/\rho)a = (W/e)_{air}.(Q/m) = 0.0087.X[R]$ in the air volume of the irradiated ionization chamber with a photon beam with X (R) under charge particle equilibrium (CPE) exposure, can be determined from the incident energy fluency $\Psi$ by means of the relationship

$$D_a[Gy] = 1.6022 \times 10^{-10} \cdot \Phi \cdot \hbar\omega \cdot \left(\frac{\mu_{en}}{\rho}\right)_a = K_{col} \qquad (17)$$

where $K_{col,a}\ [Gy] = K_a\ (1-g) = \Psi.(\mu_{en}/\rho)_a$ is the collision kerma in air. The collision kerma is the expectation value of the net energy transferred to charged particles per unit mass at the point of interest, excluding both the radiative energy loss and energy passed from one charged particle to another.

## Kerma and Absorbed Dose in Medium

**Kerma in mediu, Km**, is defined as the energy transferred from the photons to the secondary electrons per mass unit. $K_m = d(\hbar\omega)^{tr}/dm = \Psi.(\mu_{tr}/\rho)_m$ is determined by the incident energy fluency of the photons, $\Psi$, by means of the relationship,

$$K_m[Gy] = 1.6022 \times 10^{-10} \cdot \Phi \cdot \left(\frac{\mu}{\rho}\right)_m \cdot \overline{\hbar\omega}_{tr} \qquad (18)$$

where $\left(\overline{\hbar\omega}\right)_{tr}$ is the average amount of the photon energy transferred electrons in the medium.

If one compares the collision kerma between a medium 1 (for example "the air") and a medium 2, both at the same energy fluence $\Psi$, one can obtain the frequently used relation:

$$K_m = K_a \cdot \left(\frac{\mu_{en}}{\rho}\right)_{m,a} = D_a \cdot \left(\frac{\mu_{en}}{\rho}\right)_{m,a} \qquad (19)$$

**Absorbed dose in medium, Dm**, $(= d(\hbar\omega)_{en}/dm = \Psi.(\mu_{en}/\rho))$ is defined for all radiation/all media, in the charged-particle equilibrium (CPE) region beyond the dose build up maximum. It is calculatedin the same manner as kerma $\left(\overline{\hbar\omega}\right)_{en}$ except is used instead of $\left(\overline{\hbar\omega}\right)_{tr}$,

$$D_m[Gy] = 1.6022 \times 10^{-10} \cdot \Phi \cdot \left(\frac{\mu}{\rho}\right)_m \cdot \overline{\hbar\omega}_{en} = K_m(1-g) \qquad (20)$$

where $\left(\overline{\hbar\omega}\right)_{en}$ is the average kinetic energy absorbed per interaction event and Km is the total kerma in medium.

**Doza absorbita in medium $D_m$** to the same energy fluence $\Psi$, with respect to CPE in the two media is: $D_{m1} = \Psi_m.(\mu_{en}/\rho)_{m,1}$ and $D_{m,2} = \Psi_m.(\mu_{en}/\rho)_{m,2}$. From their relationship, assuming that one is air medium, results in the absorbed dose 2 (≡ m)

$$D_m[Gy] = 87 \times 10^{-4}\, X[R] \frac{(\mu_{en}/\rho)_m}{(\mu_{en}/\rho)_a} \qquad (21)$$

## Absorbed Dose in Water via Kerma

when the water phantom is irradiated with ionizing radiation, the expression for determining the absorbed dose in water, Dw, using the calibration factor for the absorbed dose to air for $^{60}$Co, $N_{D,a} = N_{K,Co}.(1\text{-}g)$ [47].

$$D_w = M \cdot N_{D,air} \cdot S_{w,air} \cdot p_\alpha \qquad (22)$$

where M is the corrected chamber signal at a point in a phantom, $s_{w,a}$ is the ratio of restricted collision stopping power of water and air and $p_\alpha$ is a perturbation correction factor.

## Neutron Absorbed Dose to Muscle Tissue

When we have a calibrated ionization chamber, the total absorbed dose in tissue from the neutron beam according to the Protocol for Neutron Dosimetry TG 18 [48] is given by

$$D_{t,T} = N_C A_{w,C} f_{t,C} d_{NG} \frac{(S_{w,g})_N}{(S_{w,g})_C} \frac{\overline{W}_N}{\overline{W}_C} \frac{K_N}{K_C} Q_T \qquad (23)$$

where : $D_{t,T}$ = total dose to muscle tissue in the neutron beam [Gy], $D_{t,T} = D_T = D_{N,G} = D_N + D_G$ ; N-neutron, G - gamma, t - total. $N_C$ = ionization chamber $^{60}$Co calibration factor (R/C) at the calibration STP (0°C = 273.15°K and 760 Torr); traceable to NBS; $Q_T$ = total corrected ionization charge (C) in the neutron beam at the standard temperature and pressure (STP) for the chamber's mass calibration. $A_{w,C}$, $f_{t,C}$, $D_{N,G}$, $(S_{w,g})_{N,C}$, $W_{N,C}$, $K_{N,C}$, factors whose values are mentioned in TG18 and one part are found in the tables.

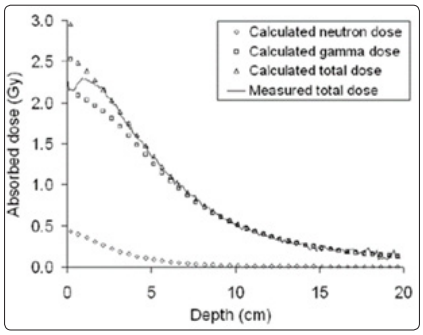


**Figure 12**: General shape of the neutron depth dose curves

The general shape of the absorbed dose distribution generated by the neutrons (calculated and measured) for therapy is presented in Fig. 12 [49].

## Interaction of electrons with matter

The major interacting processes of the secondary electrons resulting from EM radiation interactions with the substance, based on the Coulombian interaction with the orbital electrons of the atoms of the substance, are: excitation of the atom by the transfer of an orbit electron to a higher energy level and ionization of the atom by the separation of an orbital electron atom.

Both processes are considered inelastic processes, because by interaction some of the kinetic energy of the incident electron is consumed due to the binding energy of the target electron in the atom.

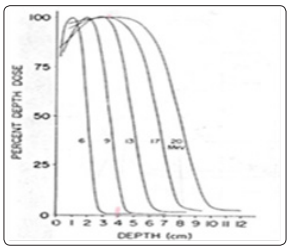


**Figure 13**: Central axis depth dose for large fields of Therac -20/ Saturne electrons [50].

The finite dose in water exposed to electron beams with the energies of 6, 9, 13, 17 and 20 MeV are shown in Fig. 13 [50].

## Mass stopping power for electron and positron

If the indirect ionization radiation has been found to be the linear mass attenuation coefficient $(\mu/\rho)[cm^2/g]$ for the direct ionization radiation, the mass stopping power$(S/\rho) \equiv dT/\rho dx$ [MeVcm$^2$/g], in which T is the kinetic energy of the electron and dx is the length of the trajectory. The unit of measurement in SI is J.m$^2$/kg or in traditionally units [MeV.cm$^2$/g]. The total mass stopping power, $(S/\rho) = (S/)_{col} + (S/\rho)_{rad}$, consists of two components: mass collision stopping power $(S/\rho)_{col}$ resulting from electron-orbital electron interactions (atomic ionizations and atomic excitations) and mass radiation stopping power $(S/\rho)_{rad}$ resulting mainly from electron - nucleus interactions (bremsstrahlung production).

Stopping powers are rarely measured, rather they are calculated from theory. The calculation formula for the mass collision stopping power for electrons and positrons is taken from the ICRU Report No. 37 [51].

$$\frac{S_{col}}{\rho} = \frac{N_A Z}{A}\frac{\pi r_0^2 2m_e c^2}{\beta^2}[\ln(KE/I)^2 + \ln(1+\tau/2) + F^{\pm}(\tau) - \delta] \qquad (24)$$

With $F^-$ given for electrons as

$$F^- = (1-\beta^2)[1+\tau^2/8-(2\tau+1)\ln 2]$$

And $F^+$ given for positrons as

$$F^+(\tau) = 2\ln 2 - (\beta^2/12)[23+14/(\tau+2)+10/(\tau+2)^2+4/(\tau+2)^3]$$

where: $N_A$-Avogadro's constant, Z-atomic number of substance, A-molar mass of substance, r0 – electron radius, $m_0c^2$ - rest mass of electron, $\beta$ = v/c, v- velocity of electron, c- velocity of light, I - mean excitation energy, $\tau$–$E_K/m_0c^2$, $\delta$ – density effect correction.

In Fig. 14 is shows the mass collision stopping power for electrons [52-53].

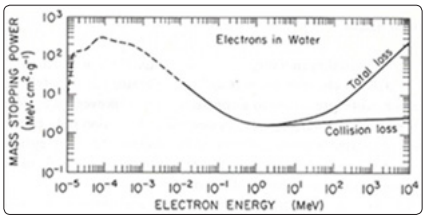


**Figure 14**: Stopping power of electrons in water as a functions of electron energy E [MeV] [52]

## Restricted stopping power for charged particles

The linear energy transfer LET or $L_\Delta$ is the energy lost T by a charged particle due to collision with electrons in traversing a unit of distance x, minus a kinetic energies of electrons in excesses of $\Delta$, $L \equiv (dT/dx)\Delta$ [43-54].

$$L_\Delta = \left(\frac{\rho}{10}\right) \times \left(\frac{dT}{\rho dx}\right)_\Delta \qquad (25)$$

The linear energy transfer $L_\Delta$ is measured, as well as the mass stopping power (S/ρ), in SI unit: J/m or in traditionally expressed in keV/μm. Both sizes represent the energy loss per unit of length.

Size L refers only to the local effects in which the energy emitted by the beam is absorbed into the elementary volume. This is achieved by limiting the energy of collisions to an imposed Δ limit, equivalent to the limitation of the trajectory of the charged particle in the elementary volume, with the purpose of eliminating from the calculation of the absorbed dose of energetic electrons δ and the nonlocal transfer of energy to the irradiated environment. In other words $(S/\rho)_{col} = \lim L_\Delta \to \infty$.

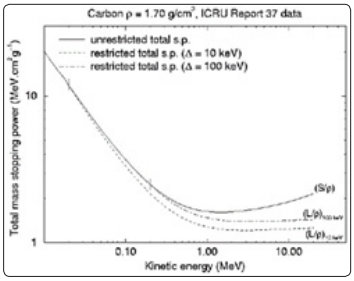


**Figure 15**: Unrestricted S/ρ and restricted ((L/ρ)Δ with Δ = 10 keV and 100 keV) [51].

In Fig. 15 is presented the total mass stopping powers for carbon, based on data published in the ICRU Report 37. Vertical lines indicate the points at which restricted and unrestricted mass stopping powers begin to diverge as kinetic energy increases. As the threshold for maximum energy transfer in the restricted stopping power.

There is research linking LET to RBE. RBE is the ratio between the dose of a reference radiation with low LET and the dose of a considered radiation that causes an identical biological effect [54].

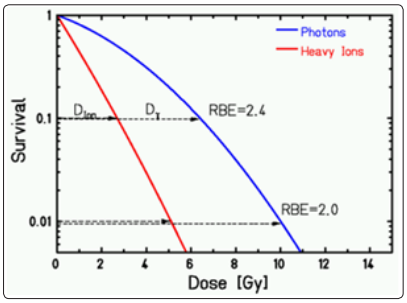


**Figure 16**: The dose response for cell survival.

The survival of a cell according to the administered dose (in the semi-logarithmic scale is presented in Fig. 16 (ICRU 2007). In this case, the RBE depends on: cell / tissue type, oxygen status, dose, dose rate and particle species. In this case $D_{eff} = D_{phy}.RBE$.

## Bragg-Gray Principle

The Bragg-Gray principle refers to the relationship between the dose absorbed in an irradiated medium and the dose absorbed in the ionization chamber cavity of sufficiently small size that does not disrupt the fluence of the secondary electrons to contribute to the dose absorbed in the ionisation chamber cavity [16].

The ionization chambers built on this principle have to meet two conditions: 1. The chamber cavity dimensions are small compared to the range of incidents charged particles and 2. The absorbed dose in the cavity is only from the charged particles that cross the cavity.

For ionization chambers meeting the Bragg-Gray conditions, the absorbed dose in the ionisation chamber cavity is given by the uniform fluence $\Phi_e^c$ of the secondary electrons released in the Bragg-Gray conditions

$$D_c = \Phi_e^c \cdot \left(\frac{1}{\rho}\frac{dT}{dx}\right)_c \qquad (26)$$

where Dc is measured in Gray dose[Gy], depending on $\Phi_e^c$ electron fluence [$cm^{-2}$] and $(S_{col}/\rho)_c \equiv (dT/\rho dx)_c$ [$MeVcm^2/g$] is the electron mass collision stopping power for the medium of density ρ for an electron at kinetic energy T.

An analogue dose in the environment surrounding the cavity is given by the same fluence of the secondary electrons, according to the relationship:

$$D_m = \Phi_e^m \left(\frac{1}{\rho}\frac{dT}{dx}\right)_m \qquad (27)$$

When the electron fluence is the same medium and the cavity, $\Phi_m = \Phi_c$, the ratio between the two absorbed dose allows to obtain the expression for the absorbed dose, for example mdiu and air.

$$D_m = D_c \cdot \left(\frac{dT}{\rho dx}\right)_m / \left(\frac{dT}{\rho dx}\right)_c = \left(\frac{Q}{m}\right) \cdot \left(\frac{W}{e}\right) \cdot s_{m,c} \qquad (28)$$

In the case of air cavity ionization chambers, the absorbed dose in the cavity air (c = a) transferred by the secondary electrons in the medium, is given by relationship

$$D_c = D_a = (W/e)\ .J_{,a}. \qquad (29)$$

Where $J_a = Q/m$ [C/kg] is the mass ionization.

Taking perturbations, the dose in the medium is determined with a thin-walled ionization chamber in a high energy photon or electron beam by:

$$D_m = \frac{Q}{m} \cdot \left(\frac{W_{gas}}{e}\right) \cdot s_{m,g}^{SA} \cdot p_n \cdot p_{dis} \cdot p_{wall} \cdot p_{cel} \qquad (30)$$

where:$S^{SA}_{mg}$ is the Spencer-Attix stopping power ratio, $(W_g/e)$ is the aveage energy expended in air per ion pair formed, $p_n$ is the electron fluence perturbation correction factor, $p_{dis}$ is the correction factor for displacement of the effective measurement point, $p_{wall}$ is the wall correction factor and $p_{cel}$ is the correction factor for the central electrode.

## Depth Dose for Hadrons

Protons and carbon ions are used in therapy due to the Bragg-Gray peak that occurs at the end range of these particles in the environment and due to the low-value constant dose of absorbed dose in adjacent tumor tissues that maintain a level until the BG peak appears.

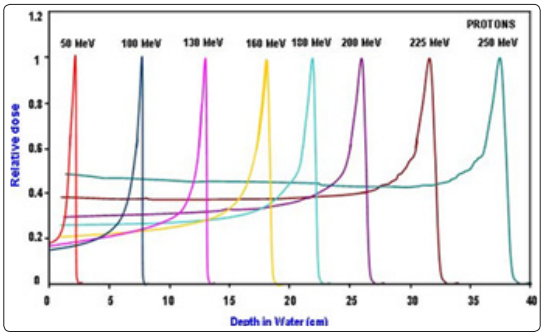


**Figure 17**: The distribution of the absorbed dose in water for protons with energy between 50 and 250 MeV.

In Fig. 17 shows the distribution of the absorbed dose in water for protons with energy between 50 and 250 MeV [55].

## Mass Stopping Power for Heavy Charged Particles

The theory of the mass collision stopping power for heavy charged particles, electrons and positrons as a result of soft and hard collisions combines the Bethe theory for soft collisions with the stopping power as a result of energy transfers due to hard collisions. The result of this, for a heavy charged particle with mass M and velocity v, where the energy transfer due to hard collisions is limited to $2\ mc^2\ \beta^2 / (1-\beta^2)$ with $\beta = v/c$, is [56].

$$\frac{S_{col}}{\rho} = \frac{N_A Z}{A}\frac{\pi r_0^2 4 m_0 c^2}{\beta^2} z^2 \left[\ln\left(\frac{2m_0 v^2}{I}\right) - \ln(1-\beta^2) - \beta^2\right] \qquad (31)$$

Where $r_0$ is the classical electron radius (2.82 fm), z is the projectile charge in units of electron charge and I is the mean excitation potential of the medium.

Collision stopping power ratio for carbon ions with energy in the clinical domain of 100-450 MeV/u is presented in Fig. 18 [57].

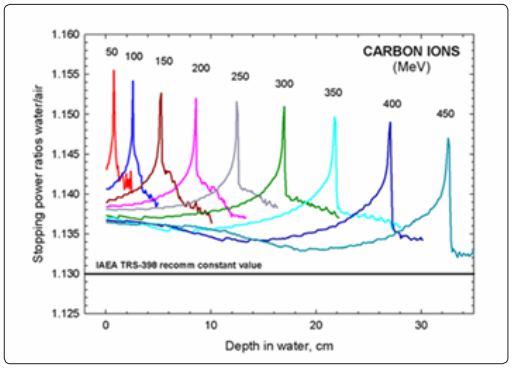


**Figure 18**: Stopping power ratio water/air for carbon ions

## Absorbed Dose for Hadrons in Other Quality Q

The absorbed dose to water in the proton or carbon ion beams of quality Q is given by relation [47]

$$D_{w,Q} = N_{D,w,Q_0} \cdot M_Q \cdot k_{Q,Q_0} \quad (32)$$

where $M_Q$ is ionization chamber reading in [C] corrected for influence quantities, $N_{D,w?Qo}$ the absorbed dose to water calibration factor of ionization chamber in a beam of quality Qo, and $k_{Q?Qo}$ the beam quality correction factor to account for the use of the calibration factor in a different beam quality Q, in our case proton or carbon ion beam, given by the relation (34)

$$k_{Q,Q_0} = \frac{(s_{w,air})_Q \cdot (W_{air}/e)_Q \cdot p_Q}{(s_{w,air})_{Q0} \cdot (W_{air}/e)_{Q0} \cdot p_{Q0}} \quad (33)$$

where $s_{w?air}$ is the water to air mass collision stopping power ratio, $(W_{air}/e)_p$ is the mean energy required to produce an ion pair in dry air and $p_Q$ is a correction factor accounting the perturbation by the presence of the ion chamber in the phantom.

The quality factor $k_{Q?Qo}$ can be measured in both qualities Q and $Q_o$ of the beam in a standard laboratory, but, due to the experimental limits, most of the times it is calculated.

The values for $k_{Q?Qo}$ were calculated and are presented in TRS 398, in function of the hadron beam quality parameter Rres. Table 1 is a synthesis of the parameters of the component formula $k_{Q?Qo}$ factor.

**Table 1: Specific factors for Q hadron beams and for the Qo calibration beam**

| $k_{Q,Q_o}$ parameter | Value for protons | Values for carbon ions |
|---|---|---|
| $(s_{w,air})_{Qo}$ | 1.133 | 1.133 |
| $(s_{w,air})_{Q}$ | Function of E | Function of E |
| $(W_{air}/e)_{Qo}$ | 33.97 eV | 33.97 eV |
| $(W_{air}/e)_{Q}$ | 34.50 eV | 34.23 eV |
| $p_{Qo}$ | 1.009 | 1.009 |
| $p_Q$ | 1.0 | 1.0 |

## Equivalent Dose and Effective Dose Limits

In the field of radiobiology and radiotherapy, it is necessary to know the absorbed dose within a tissue or organ. In this respect, ICRP Publication 60 recommends the concept of tissue or organ absorbed dose $D_T$, defined as the quotient of $E_T$ by $m_T$, where $E_T$ is the total amount of energy deposited in the organ or tissue and $m_T$ is the mass of the organ or tissue, $D_T=E_T/m_T$. The absorbed dose measurement unit is the Gray (1Gy = 1J/kg = 6.24 x $10^9$ MeV/g =$10^4$ erg/g = 100 rad (radiation absorbed dose).

The equivalent dose in any tissue or organ ($H_{T,R}$) is the product of tissue absorbed dose and radiation weighting factor ($w_T$) for radiation R, i.e. $H_T = w_R \bullet D_{T,R}$ where $D_{T,R}$ is the average absorbed dose in tissue T from radiation R. When more than one radiation type is involved, the total equivalent dose in each tissue or organ is $H_T = \Sigma_R w_R \bullet D_{T,R}$ [53].

The radiation weighting factors for radiation types and energy ranges are the following. For light particles (X and γ rays, electrons, positrons and muons, all energies) the radiation weighting factor $w_R$ = 1. For heavy particles $w_R$>5. Among these we mention: protons: $w_R$ = 5 (> 2 MeV), neutrons: $w_R$ = 5 (< 10 keV), $w_R$ = 10 (10-100 keV), $w_R$ = 20 (>100 keV - 2 MeV), $w_R$ = 10 (2-20 MeV), $w_R$ = 5 (> 20 MeV) and alpha particles, fission fragments and heavy nuclei, $w_R$ = 20.

The effective dose E is defined (ICRP 91) as the sum of equivalent doses to organs and exposed tissue, each multiplied by the appropriate tissue weighting factor $w_T$ (0.01/skin - 0.20/gonads), $E = \Sigma_T w_T \bullet H_T = \Sigma_T w_T \bullet \Sigma_R w_R D_{T,R}$. Measurement unit for doses $H_T$ and E is Sievert, abbreviated as Sv, 1 Sv = 100 rem - (roentgen equivalent man).

ICRP recommended anual dose limits for occupational personell/ general public, the effective dose E for whole body: 20 [mSv/1mSv] and the equivalent dose H for lens: 150/15 [mSv/mSv], skin 500/50 [mSv/mSv] and hands & feet 500 [mSv]. Note that such limits exclude any medical or natural background radiation doses.

The dose limits recommended for exposure cases planned for equivalent dose for personnel working in the radiation domain and for members of the public is shows in Fig.19. Moreover, the levels of the dose equivalent for the internal and external natural irradiation as well as for the internal and external artificial irradiation are presented [58].

ICRP recommends for whole body E = 20 mSv for occupational personal and E = 1 mSv for general public, $H_T$= 150 mSv for occupational and 15 mSv for general public, for skin $H_T$ = 500 mSv.

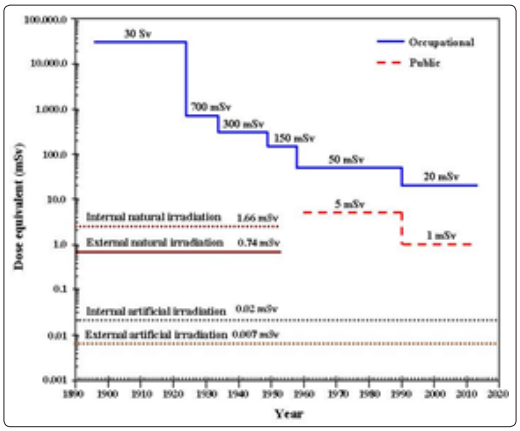


**Figure 19**: Recommended and natural dose limits adapted from [58].

## Conclusion

The principle of dosimetry with the ionization chamber for determining the absorbed dose applies to all kinds of radiation and materials, since the cavities of the electronic equilibrium ionization chambers respond to the electrons released inside the cavity, and the cavities of the Bragg-Gray chambers respond to electrons released outside the cavity ($\mu_{en}/\rho$).

The principle of charged particle equilibrium (CPE) links the absorbed dose into the large cavity ionization chamber and the absorbed dose in the irradiated medium containing the ionization chamber. The energy fluence $\Psi$ of the radiation field is a common factor in determining the three dosimetric sizes at the point where CPE exists, as follows: $D = \Psi.(\mu_{en}/\rho)$, $K = \Psi.(\mu_{tr}/\rho)$, $K_{col} = \Psi.(\mu_{en}/\rho)$, and $X = \Psi.(1/\Psi_R)$, where the multiplication is done with the inverse of the incident energy fluence, $\Psi_R$, of the 1 R radiation field.

The Bragg-Gray principle links the dose absorbed into the small-sized air cavity and thin walls and the absorbed dose in the irradiated medium containing the ionization chamber. For this use the secondary electrons fluence $\Phi_e$ generated in the irradiated medium. The absorbed dose is equal to the secondary electron fluency multiplied by the electron energy collision stopping power $(S/\rho)_{col}$, $D = \Phi_e.(S/\rho)_{col}$.

The use of mechanisms to accelerate the hadrons using laser technology to the energies required for radiotherapy (50-250) MeV for protons and (100-450) MeV /u for carbon ions by means of the laser electric field instead of RF electric field will lead to the multiplication of hadron therapy in order to benefit as many patients as possible from these treatments.

## References


1. Bevalacqua J. J. (2007) Health Physics in the 21st Century, WILEY-VCH Verlag GmbH & Co. KGaA.
2. Amaldi U, R. Bonomi, S. Braccinin, M. Crescenti, A. Degiovanni, et al. (2010) Accelerators for hadrontherapy: From Lawrence Cyclotrons to Linacs, Nucl. Instr. and Meth.in Phys. Res. A 620: 563-577.
3. Scarlat F, Stancu E, Badita E, Scarisoreanu A, Vancea C, et al. (2017) Detection and Absorbed Dose Determination in Clinical Radiation Fields, Proc. of the 3rd Int. Conference on Sensors and Electronic Instrumentation Advances 113-118.
4. Scarlat F, Scarisoreanu A, Badita E, Vancea C, Calina I, et al. (2015) Ionization Chamber Dosimetry for Conventional and Laser - Driven Clinical Hadron Beams, Journal of Biosciencis and Medicines 3: 8-17.
5. Badita E, Vancea C, Calina I, Stroe D, Dumitrache M, et al. (2017) Long term stability of the performance of a clinical linear accelerator and z-score assessment for absorbed dose to water quantity, Romanian Reports in Physics vol. 69: 606.
6. Stancu E, Vancea C, Valenta J, Zeman J, Badita E, et al. (2015) Assessment of absorbed dose to water in high energy photon beams using different cylindrical chambers, Romanian Reports in Physics 67: 693-699.
7. Macchi A, Borghesi M, Passoni M (2013) Rev. Mod. Phys 85: 751.
8. Robinson A.P.L, Gibbon P, Zepf M, Kar S, Evans R.G, et al. (2009) Relativistically correct hole boring and ion acceleration by circularly polarized laser pulses, Plasma Phys. Control. Fusion 51, 024004.
9. Bulanov S.V, Khoroshkov V.S (2002) Feasibility of Using Laser Ion Accelerators in Proton Therapy, Plasma Physics Reports 28: 453-456.
10. Stancu E, Badita E, Scarlat F, Scarisoreanu A, Scarlat F(2014) Evaluation of quality factor for clinical proton beams, Romanian Reports in Physics 66: 192-199.
11. Stancu E, Vancea C, Valenta J, Zeman J, Badita E, et al. (2015) Absorbed dose to water measurements in high energy electron beams using different plane parallel chambers, Romanian Reports in Physics 67: 1152-1158.
12. Scarisoreanu A, Scarlat F, Stancu E, Badita E, Dumitrascu M, et al. (2017) Absorbed dose to water and air kerma results for measurements carried out in an oncology radiotherapy laboratory, Romanian Reports in Physics 69: 605.
13. Stancu E, Kapsch R.P, Badita E.S, Scarlat F, Scarisoreanu A.M (2018) The equivalence of the absorbed dose to water in high energy photon beams 12: 237-239.
14. Scarlat F, Scarisoreanu A, Minea R, Badita E, Sima E, et al. (2013) Secondary Standard Dosimetry Laboratory at INFLPR, Optoelectronics and Advanced Materials - Rapid Communications 7: 618-624.
15. Attix F. R, Roesch W.C, Tochilin E (1968) Radiation Dosimetry, Second Edition, Vol. I, Fundamentals (Academic Press, New York).
16. Case K. R, Nelson W. R (1972) Concepts of Radiation Dosimetry, SLAC 153 UC 34, MISC.
17. International Commission on Non-Ionizing Radiation Protection ICNIRP (1998), Publication - 1998, ICNIRP Guidelines for limiting Exposure to Time-Varying Electric, Magnetic and Electromagnetic Fields (up to 300GHz), Health Physics 74: 494-522.
18. Johnson C. C, Guy A. W (1972) Non ionizing Electromagnetic Wave Effects in Biological Materials and Systems, Proc. IEEE 6: 692-718.
19. Al-Ghazi M. S. A. L, Arjune B, Fiedler J. A, Sharma P. D (1988) Dosimetric aspects of the therapeutic photon beams from a dual - energy linear accelerator, Med. Phys 15: 250-257.
20. Gibbon P (2011) Physics of High Laser Plasma Interactions, Varena Summer School on Laser Plasma Acceleration 6-132.
21. Saldin E. L, Schneidmiller E.A, Yurkov M. W (2006) Coherence properties of the Radiation from X-ray free electron laser, DESY 288: 1179-1188.
22. Sprangle P, Ting A, Esarey E, Fisher A (1992) Tunable short pulse x-rays from a compact laser synchrotron source, J. Appl. Phys 72: 5032-5038.
23. Scarlat F, Oproiu C (1994) The 40 MeV Medical Betatron. Experience versus Predictions, Proceedings of the Fourth European Particle Accelerator Conference (EPAC-94), London, England 3: 2616- 2618.
24. Scarlat F, Scarlat Fl (2002) A Potential X Ray Laser Synchrotron Source for Small Laboratories", Proc of the 27 ARA Congress, (ARA-27), Oradea, Romania.
25. Chernyaev A. P, Varzar S. M (2014) Particle Accelerators in Modern World, Physics of Atomic Nuclei 10: 1203-1215.
26. Lawrence E.O (1932) Method and Apparatus for Acceleration for Ions, Fied Jan 20, 1932, US Patent Office, Serial No. 589033.
27. Craddock M. K (2011) Cyclotrons: from Science to Human Health and Triumf, American Physical Society, April Meeting 2011, Anaheim, CA.
28. Yves Jongen (2010) Review of cycloyrons for cancer therapy, FRM1CIO01, Proceedings of CYCLOTRONS 2010, Lanzhou,

China 398- 403.
29. Röcken H, Abdel-Bary M, Akcöltekin E, Budz P, Stephani T, et al. (2010) The VARIAN 250 MeV Superconducting Compact Proton Cyclotron: Medical Operation of the 2nd Machine, Production and Commissioning Statutus of Machines No. 3 to 7, Proceedings of Cyclotrons 2010, Lanzhou, China TUM1CCO04: 283-285.
30. Morozov N (2010) IBA-JINR 400 MeV/u Superconducting Cyclotron for Hadron Therapy, FRM1CIO03, Proceedings of CYCLOTRONS 2010, Lanzhou, China 398-403.
31. Coutrakon G (2007) Accelerators for Heavy-charged-particle Radiation Therapy, Technology in Cancer Research & Treatment, Volume 6, Number 4 Supplement 6: 49-54.
32. Scarlat F, Scarisoreanu A, Verga N, Scarlat Fl (2015) "Laser - Driven Hadron Therapy Project", International Conference on Accelerators and Large Experimental Physics Control Systems, ICALEPCS 2015, Melbourne, Australia.
33. Carrigan R.A. Jr (1982) On the possible applications of the steering of charged particles by bent single crystals including the possibility of separated charm particle beams 194: 205-208.
34. Badita E, Vancea C, Stancu E, Scarlat F, Calina I, et al. (2016) Study on the development of a new single mode optic fiber radiation dosimeter for electron beams, Romanian Reports in Physics 68: 604-614.
35. Badita E, Stancu E, Vancea C, Scarlat F, Calina I, et al. (2015) Influence of high energy ionizing radiation on single mode optical fiber proprieties, The third international conference on radiation and applications in various fields of research 41-45.
36. Zamfir N.V (2012) Extreme Light Infrastructure - Nuclear Physics ELI-NP, Experimental Programme Workshop at ELI-NP, Bucharest.
37. Verga N, Ursu I, Craciun L, Mirea D. A, Vasilescu R, et al. (2014) Eye proton therapy: proposed feasibility plan SF, Romanian Reports in Physics 66: 223-246.
38. T. Esirkepov, M. Borghesi, S. V. Bulanov, G. Mourou, T. Tajima (2004) Highly Efficient Relativistic-Ion Generation in the Laser-Piston Regime, Phys. Rev. Lett 92: 175003.
39. Esirkepov T, Yamagiva M, Tajima T (2006) Laser Ion Acceleration laws Scaling Seen Multiparametric Particle-in-cel Simulation, Phys. Rev. Lett 96: 105001.
40. Scarlat F, Scarisoreanu A, Verga N, Scarlat Fl, Vancea C (2014) "Towards Laser Driven Hadron Cancer Radiotherapy: Journal of Intense pulsed Lasers and Applications in Advances Physics 4: 55-64.
41. Scarlat F, Verga N, Scarisoreanu A, Badita E, Dumitrascu M, et al. (2013) Journal of Intense Pulsed Lasers and Applications in Advanced Physics 3: 15-25.
42. Fitzgerald J. J, Brownell G. L, Mahoney F. J. (1967) Mathematical Theory of Radiation Dosimetry (Gordon and Breach, New York).
43. Dance D. R, Christofides S, Maidment A.D.A, McLean I. D, K. H. Ng (2014) Diagnostic Radiology Physics, A Handbook for Teachers and Students, IAEA Vienna.
44. Martin J. E. (2006) Physics for Radiation Protection A Handbook, WILEY-VCH Verlag GmbH & Co. KGaA.
45. Turner J. E. (2007) Atoms, Radiation, and Radiation Protection, WILEY-VCH Verlag GmbH & Co. KGaA.
46. Evans R.D (1955) The Atomic Nucleus, McGraw-Hill Book Company, Inc., New York 2: 11s-12s.
47. IAEA TRS 398 (2000) Absorbed dose determination in external beam radiotherapy. An international code of practice for dosimetry based on standards ao absorbed dose to water. Tehnical Report no 398.
48. AAPM Report No 16 (1966) Protocol for heavy Charged particle Therapy beam dosimetry, A Report of Task group 20 Radiation Therapy Committee American Association of Physicists in Medicine, American Institute of Physics, New York 10017.
49. https://www.google.ro/ search?q=depth+dose+in+water+for+neutrons.
50. Sharma S. C, Wilson D. L (1985) Depth dose characteristics of elongated fields from electron beams from a 20 MeV accelerator, Med. Phys 12: 419-423.
51. ICRU Report 37 (1984) Stopping Powers for Electrons and Positrons, International Commission on Radiation Units and Measurements, Bethesda, MD, USA.
52. IAEA, TRS 188 (1979) Radiological safety Aspects of the operation of Electron Linear Accelerator, Vienna.
53. ICRU Report 21 (1971) Radiation Dosimetry: Electrons with initial energies Between 1 and 50 MeV, International Commission on Radiation Units and Measurements, Washington D.C, USA.
54. ICRP, 1991b. 1990 Recommendations of the International Commission on Radiological Protection. ICRP Publication 60, ann. ICRP 21 (1-3).
55. The normalized (at peak) Bragg Curves for Various Proton Incident Energies in Water Phantom: A simulation with GEANT4 Monte Carlo Code, Abstract ID 8159, www.aapm.org/meetings/amos2/pdf.
56. Berger M. J, S.M.Seltzer (1983) Stopping Powers and Ranges of Electrons and Positrons, NBSIR 82-2550-A, NBS - DC, U.S.A.
57. Geithner O, Andreo P, Sobolevsky N, Hartman G, Jakel O (2006) Calculating of stopping power ratios for carbon ions dosimetry, Phys. Med. Biol 51: 2279-2292.
58. Inkret W. C, Meinhold C. B, Tascher J. C (1995) A Brief History of Radiation Protection Standards, Los Alamos Science 23: 116-123.